NANO LETTERS

Letter

pubs.acs.org/NanoLett

High Energy Density Asymmetric Quasi-Solid-State Supercapacitor Based on Porous Vanadium Nitride Nanowire Anode

Xihong Lu,[†,‡] Minghao Yu,[†] Teng Zhai,[†] Gongming Wang,[‡] Shilei Xie,[†] Tianyu Liu,[‡] Chaolun Liang,[†,§] Yexiang Tong,*[,†] and Yat Li*[,‡]

[†]KLGHEI of Environment and Energy Chemistry, MOE of the Key Laboratory of Bioinorganic and Synthetic Chemistry, School of Chemistry and Chemical Engineering, Sun Yat-Sen University, Guangzhou 510275, People's Republic of China

[‡]Department of Chemistry and Biochemistry, University of California, Santa Cruz, Santa Cruz, California 95064, United States

[§]Instrumental Analysis and Research Centre, Sun Yat-Sen University, Guangzhou 510275, People's Republic of China

Supporting Information

ABSTRACT: To push the energy density limit of asymmetric supercapacitors (ASCs), a new class of anode materials is needed. Vanadium nitride (VN) holds great promise as anode material for ASCs due to its large specific capacitance, high electrical conductivity, and wide operation windows in negative potential. However, its poor electrochemical stability severely limits its application in SCs. In this work, we demonstrated high energy density, stable, quasi-solid-state ASC device based on porous VN nanowire anode and VO_x nanowire cathode for the first time. The VO_x//VN-ASC device exhibited a stable electrochemical window of 1.8 V and excellent cycling stability with only 12.5% decrease of capacitance after 10 000 cycles. More importantly, the VO_x//VN-ASC device achieved a high energy density of 0.61 mWh cm^{-3} at current density of 0.5 mA cm^{-2} and a high power density of 0.85 W cm^{-3} at current density of 5 mA cm^{-2}. These values are substantially enhanced compared to most of the reported quasi/all-solid-state SC devices. This work constitutes the first demonstration of using VN nanowires as high energy anode, which could potentially improve the performance of energy storage devices.

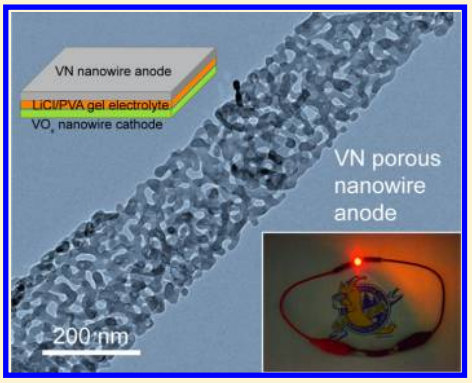

KEYWORDS: *Asymmetric supercapacitors, nanowires, vanadium nitride, anode*

As the electricity consumption by electronic devices and electric vehicles continues to grow, it urges the development of novel energy storage devices with high power and energy density.[1−8] Flexible quasi/all-solid-state supercapacitors (SCs) are emerging as one of the most promising energy-storage devices due to their outstanding properties such as high power density, fast charge/discharge capability, light weight, ease of handing, and excellent reliability over a wide range of operating temperatures.[9−12] These unique features enable them to be potentially used as power sources for portable and flexible electronics, paper-like personal gadgets, and miniature biomedical devices, etc.[13−15] However, for practical applications, it is essential to increase the energy density and operating voltage of quasi/all-solid-state SCs, without sacrificing the device power density and cycle life. A promising strategy to increase the energy density and cell voltage is to develop asymmetric quasi/all-solid-state supercapacitors (ASCs).[7,9,16,17] ASCs are mostly consisting of a battery-type Faradic electrode (cathode) as energy source and a capacitor-type electrode (anode) as power source.[7,9,16−19] ASCs take advantage of different potential windows of the two electrodes to increase the device operating voltage (up to 2.0 V) and hence significantly improve the energy density.

Despite great progress having been made in improving the capacitance of cathode materials, the anode material is rarely studied. Carbon-based nanomaterials are commonly used as anode in ASCs because of their high surface area, excellent electrical conductivity, and large power density.[7,9,16,18,19] However, the low specific capacitance of carbon materials severely limits the energy density for ASCs. It is highly desirable to explore new anode materials. Metal oxide based anodes such as MoO_{3-x}[17] and iron oxide[20] have shown much higher energy density than carbon-based materials; however, they suffered from limited power density due to their poor electrical conductivities. Vanadium nitride (VN) holds great promise as anode for ASCs due to its large specific capacitance (1340 F g^{-1}) and high electrical conductivity (σ_{bulk} = 1.67 × 10^6 Ω^{-1} m^{-1}). More importantly, VN has a suitable working window in negative potential for anode.[21−25] Yet, VN anode is electrochemically instable in aqueous solution due to the irreversible electrochemical oxidation reaction of forming vanadium oxide (VO_x) on the surface.[22−24] While the formed VO_x is electrochemically active and could improve the

Received: February 28, 2013
Revised: April 13, 2013
Published: May 1, 2013

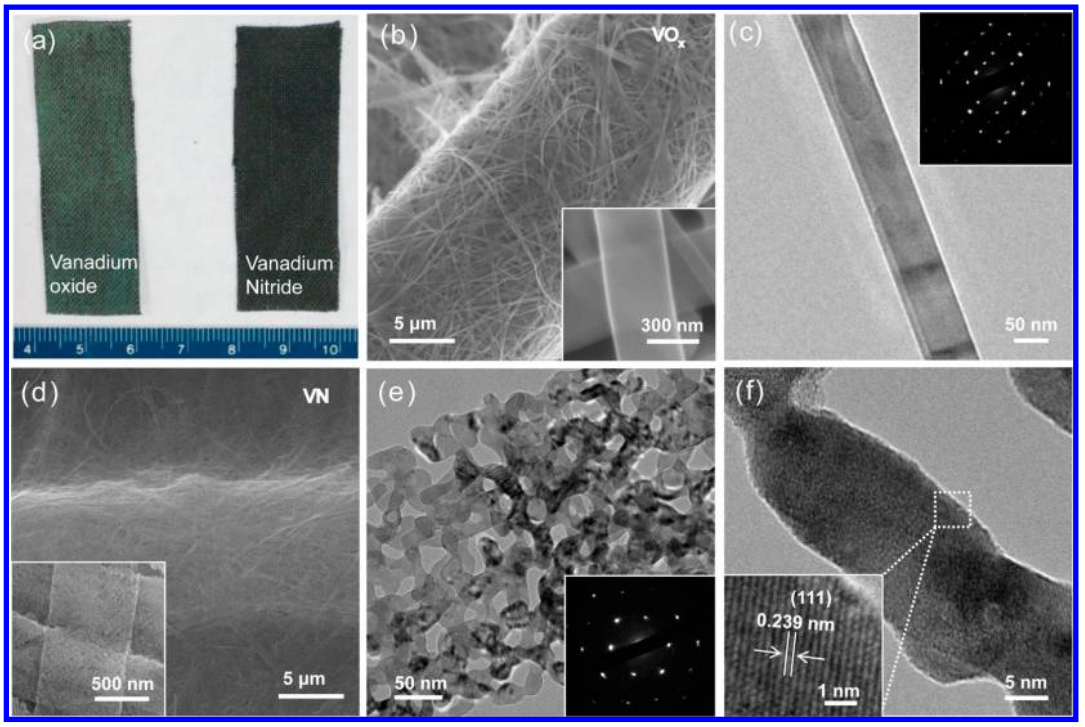

Figure 1. (a) Digital micrograph of carbon cloth substrates coated with VO_x and VN nanowires. (b) SEM image of VO_x nanowires grown on carbon cloth substrate. Inset: magnified SEM image of the nanowires. (c) TEM image of a VO_x nanowire. Inset: corresponding SAED pattern. (d) SEM image of VO_x nanowires thermally annealed in ammonia (VN nanowires). Inset: magnified SEM image of the nanowires. (e) TEM image of a porous VN nanowire. Inset: corresponding SAED pattern. (f) Magnified TEM image collected at the edge of the porous nanowire. Inset: lattice-resolved TEM image.

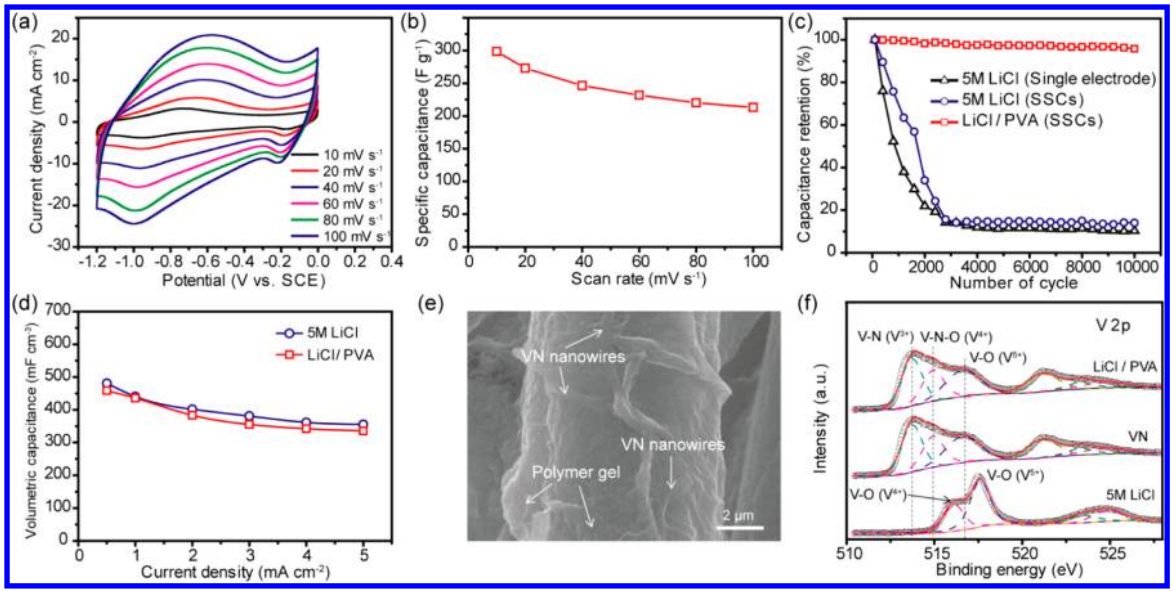

Figure 2. (a) CV curves and (b) specific capacitance of VN nanowire electrode collected at various scan rates. (c) Cycling performance of single VN electrode and symmetric VN SC devices collected at a scan rate of 100 mV s^{-1} for 10 000 cycles in 5 M LiCl aqueous electrolyte and LiCl/PVA gel electrolyte. (d) Volumetric capacitance calculated from the galvanostatic charge−discharge curves as a function of current density in LiCl aqueous electrolyte and LiCl/PVA gel electrolyte. (e) SEM image of VN nanowires embedded in LiCl/PVA gel electrolyte after testing for 10 000 cycles. (f) Core level V 2p XPS spectra collected for VN nanowires before and after testing for 10 000 cycles in LiCl aqueous electrolyte and LiCl/PVA gel electrolyte. Empty circles are the experimental results. The red curves are the summation of the fitting curves (dashed curves).

electrochemical performance of VN and prevent VN surface from further oxidation, VO_x is soluble in aqueous solution. The poor electrochemical stability of VN causes severe capacitance loss during charging/discharging cycling process.[21,26] For instance, VN nanoparticles grown on carbon nanotubes retained about 60% of their initial capacitance after 600 cycles in 1 M KOH electrolyte.[24] Nanocrystalline VN electrode with an ultrahigh specific capacitance of 1340 F g^{-1} has been recently developed. However, it retained 90% of its initial capacitance after 1000 cycles in 1 M KOH solution.[21]

In this work, we demonstrated high energy density, asymmetric quasi-solid-state supercapacitors based on porous

dx.doi.org/10.1021/nl400760a | *Nano Lett.* 2013, 13, 2628−2633

VN nanowire anode. Anode based on porous VN nanowire arrays grown on carbon cloth substrate not only offers good conductivity and high surface area but also avoids the use of binder. The stability of the VN nanowire anode was significantly improved by using a LiCl/PVA gel electrolyte, which retains more than 95% of initial capacitance after 10 000 cycles. The success of stabilizing VN nanowires in a LiCl/PVA gel electrolyte also offers new opportunities in design and fabrication of high-performance ASC devices. Here we demonstrate a quasi-solid-state ASC device based on VN nanowire anode and VO_x nanowire cathode achieved a remarkable volumetric energy density of 0.61 mWh cm^{-3}, which is higher than most of reported quasi and all-solid-state SCs.[1,5,9,12,15,16,26,27]

Porous VN nanowires were fabricated through a two-step approach. First, VO_x nanowires were grown on a carbon cloth substrate by the hydrothermal method reported elsewhere (Experimental Section, Supporting Information),[26] followed by postannealing in ammonia at 600 °C for 1 h. The digital image (Figure 1a) shows that carbon cloth substrates covered by VO_x and VN nanowires are green and black in color. The hydrothermal growth method enables uniform growth of nanowires over the entire substrate. Scanning electron microscopy (SEM) images reveal that individual carbon fibers were uniformly wrapped by interlaced VO_x nanowires (Figure 1b). The average diameter of VO_x nanowires is between 300 and 800 nm, while the length is up to tens of micrometers. The transmission electron microscopy (TEM) image shows that the VO_x nanowire is uniform in diameter with smooth surface. Selected area electron diffraction (SAED) diffraction pattern confirmed that the VO_x nanowire is a single crystal (Figure 1c). Powder X-ray diffraction (XRD) analysis proved that the VO_x nanowires were successfully transformed into cubic VN nanowires (Figure S1, Supporting Information). The SEM image (Figure 1d) shows that the nanowire-like morphology was essentially preserved after nitridation. Interestingly, TEM studies further revealed that the VN nanowires are single crystalline porous structures (Figure 1e). The lattice-resolved TEM image collected at the edge of the porous structure revealed a lattice fringe of 0.239 nm that is consistent with the *d*-spacing of (111) plane of the cubic VN structure.

The electrochemical properties of the porous VN nanowires were examined in a three-electrode cell using 5 M LiCl aqueous solution as electrolyte, a Pt wire as counter electrode, and an Ag/AgCl electrode as reference electrode. The mass loading of VN nanowires on carbon cloth was about 0.71 mg cm^{-2}. Figure 2a shows the cyclic voltammograms (CV) collected for porous VN nanowire electrode in a potential window between −1.2 and 0 V at different scan rates. The CV curves present essentially the same shape as the scan rate increases from 10 to 100 mV s^{-1}, indicating the good capacitive behavior of VN nanowires. The VN nanowire electrode achieved an excellent specific capacitance of 298.5 F g^{-1} (for detailed calculation see Supporting Information) at the scan rate of 10 mV s^{-1} (Figure 2b), which is substantially higher than that of conventional carbon-based electrodes[2,19,28,29] as well as recently reported VN nanostructured electrodes.[23−25,30] Furthermore, VN electrode exhibited excellent rate capability, with a retention rate of 71.5% when the scan rate increased from 10 to 100 mV s^{-1}, which is higher than that of nanocrystalline VN particles[21,22] and comparable to other VN nanostructures.[23,24,30] The superior electrochemical performance of VN nanowires can be attributed to the large accessible surface area of the porous structure, low interfacial resistance as a result of direct contact between carbon cloth substrate and VN nanowires (without the need of binder). However, the VN nanowire electrode suffered from a poor cycling stability in aqueous solution, which is consistent with the previous studies.[22−25] As shown in Figure 2c, the capacitance of VN electrode decreases continuously in aqueous solution, and only about 10% of the initial capacitance was retained after 10 000 cycles. XPS analyses indicated that the VN nanowires were oxidized to VO_x after cycling measurement (Figure 2f and Figure S2). Moreover, the insertion/extraction of Li^+ into cubic VN would lead to the formation of a solid solution since the cubic VN does not have rigid layered structure, and it seems not likely for the structural recovery of the cubic phase from the solid solution.[31,32] In addition, SEM images revealed the coverage of nanowires on carbon cloth substrate was significantly lower after 10 000 cycles (Figure S3). Therefore, the instability of VN electrode was due to irreversible oxidation reaction, irreversible phase change, and the detachment of nanowires from substrate. It is clear that a substantial improvement of the electrochemical stability of VN nanowires is needed.

Our strategy to improve the stability of VN nanowires was to use LiCl/PVA gel electrolyte. We have recently demonstrated that LiCl/PVA gel electrolyte can prevent the chemical dissolution of vanadium oxides by minimizing the water content and avoid structure pulverization of vanadium oxides by holding the direct contact between electrochemically active materials and substrate during cycling.[26] We hypothesized that this neutral gel electrolyte with limited amount of water can also effectively suppress the electrochemical oxidation reaction of VN nanowires and increase their mechanical stability. We fabricated SSCs based on the as-prepared VN nanowires (Experimental Section) and investigated their cycling stability in both a 5 M LiCl aqueous solution and a LiCl/PVA gel electrolyte. Significantly, the LiCl/PVA gel electrolyte prominently improved the stability of VN electrode, with an extremely high capacitance retention of 95.3% after 10 000 cycles (Figure 2c). This is the best cycling performance reported for VN nanostructures. More importantly, the VN electrode measured in LiCl/PVA gel electrolyte and 5 M LiCl aqueous electrolyte showed similar electrochemical behavior (Figure S4) and volumetric capacitance (Figure 2d and Figure S5; for a detailed calculation see Supporting Information) at various current densities, indicating the ion diffusions are equally efficient in both electrolyte medium. Electrochemical impedance spectroscopy measurements further showed that the corresponding time constant t_0 ($=1/f_0$) for the VN SSCs with gel electrolyte is 0.27 s, which is comparable to the value of 0.38 s obtained in aqueous electrolyte (Figure S6; for details see Supporting Information). These rapid frequency responses obtained for the VN SSCs support the efficient mass transport in both gel and aqueous electrolyte. Furthermore, there is no obvious change in the nanowire morphology after testing for 10 000 cycles (Figure 2c). Core level V 2p and N 1s spectra also showed that the compositional modification of VN electrode was minor (Figure 2f and Figure S2). These results confirmed our hypothesis that the LiCl/PVA gel electrolyte can effectively suppress the irreversible oxidation reaction and structural pulverization of VN nanowires, without sacrificing their electrochemical performances.

The success of stabilizing VN nanowires in the LiCl/PVA gel electrolyte offers new opportunities in using VN nanowires as high energy anode (vs conventional carbon materials) for

dx.doi.org/10.1021/nl400760a | *Nano Lett.* 2013, 13, 2628−2633

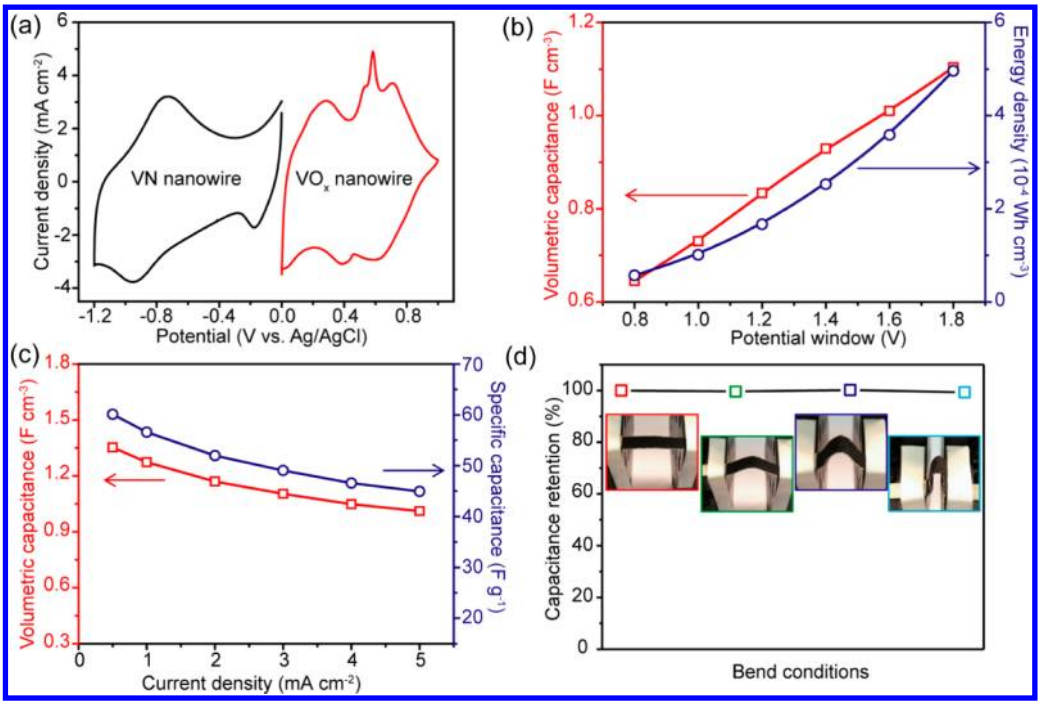

Figure 3. CV curves collected for VN and VO_x nanowire electrodes at a scan rate of 10 mV s^{-1}. (b) Volumetric capacitance and energy density calculated for the VO_x//VN-ASC device based on galvanostatic charge−discharge curves collected at 4 mA cm^{-2} as a function of potential window. (c) Volumetric capacitance and specific capacitance calculated for the VO_x//VN-ASC device based on the galvanostatic charge−discharge curves as a function of current density. (d) Capacitance retention of the VO_x//VN-ASC device measured at different bent conditions. Insets: pictures of the device.

ASCs. We fabricated ASC devices by using VN nanowires as anode and VO_x nanowires as cathode (denoted as VO_x//VN-ASC). CV curves and specific capacitance for VO_x nanowires collected at different scan rates are shown in Figure S7. In order to obtain the maximum performance of the ASC device, the charge between the positive and the negative electrodes should be balanced.[17,19] The mass ration between the VO_x electrode and VN electrode is about 1.65:1 (for details, see the Supporting Information). Taking advantage of the different potential windows of VN and VO_x electrodes (Figure 3a), it was expected that the operating cell potential can be extended to 2.2 V when they are assembled into ASCs. However, a Faradic reaction was observed in the CV and charge−discharge curves beyond the potential of 1.8 V (Figure S8). This Faradic reaction could be ascribed to the electrochemical oxidation of VN electrode. When the ASC devices were tested in the potential windows of 2 and 2.2 V for 10 000 cycles, their capacitances dropped more than 61% and 84%, respectively (Figure S9). In contrast, the ASC device exhibited excellent cycling stability with only 12.5% decrease of capacitance after 10 000 cycles, when it was operated in a potential window between 0 and 1.8 V. The cell capacitance depends on the capacitance of VN anode and VO_x cathode.[9,17] The capacitance of VN nanostructured electrode is a combined contribution of electrical double-layer capacitance and pseudocapacitance due to the Faradic reactions occur on the surface of VN.[21,24,30] XPS analyses (Figure 2f) revealed the presence of a small amount of vanadium oxide and vanadium oxynitride on the VN nanowire surface. Therefore, the possible Faradic reations in LiCl electrolyte can be described as follows:

$$V_{x+2y/3}N_xO_y + zM^+ + ze^- \leftrightarrow V_{x+(2y-z)/3}N_xO_yM_z^{z+}$$
$$(M^+ = Li^+, H^+)$$

For the VO_x cathode capacitance, it mainly arises from the pseudocapacitance due to reversible redox transitions involving the insertion/extraction of protons and/or Li^+ ions as well as the transitions between different valence state of V.[33,34] The possible reaction mechanism is expressed as follows:

$$VO_x + yM^+ + ye^- \leftrightarrow V_{2x-y}O_xM_y^{y+} \quad (M^+ = Li^+, H^+)$$

To confirm this mechanism, more detailed investigations are needed, which is not the scope of this work. Figure 3b shows the volumetric capacitance (based on the volume of the entire device) of the ASCs measured at 4 mA cm^{-2} at different operation potentials from 0.8 to 1.8 V. As expected, the volumetric capacitance dramatically increases from 0.65 to 1.1 F cm^{-3} as the operation potential increases from 0.8 to 1.8 V. Meanwhile, the volumetric energy density of the ASC was also greatly improved from 0.057 to 0.50 mWh cm^{-3} with an enhancement more than 800%.

To further study the electrochemical performance of the ASC device, CV curves and galvanostatic charge−discharge curves were collected for the VO_x//VN-ASC device at various scan rates and current densities, in a range of potential windows between 0 and 1.8 V. These CV curves exhibited rectangular-like shapes without obvious redox peaks, even at a scan rate of 200 mV s^{-1}, indicating outstanding capacitive behavior and fast charge/discharge property (Figure S10). Additionally, the triangle shape of charge−discharge curves also confirmed the excellent capacitive behavior of the ASC device (Figure S11). The ASC device achieved a volumetric capacitance (based on the volume of the entire device) of 1.35 F cm^{-3} (60.1 F g^{-1},

dx.doi.org/10.1021/nl400760a | Nano Lett. 2013, 13, 2628−2633

based on the total mass of active materials) at current density of 0.5 mA cm^{-2}, which is considerably higher than the values obtained from recently reported quasi/all-solid-state SSCs and ASCs at the same current density (Figure 3c).[1,5,9,12,13,15,26,27] The ASC device also demonstrated a remarkable rate capability, which retained about 74.7% of the initial capacitance (1.01 F cm^{-3}, 44.9 F g^{-1}) as the scan rate increased from 0.5 to 5 mA cm^{-2}. Moreover, the ASC device has excellent mechanical flexibility. The folding and twisting of the device do not affect its electrochemical performance (Figure 3d), which ensures it to be potentially used as flexible energy storage device.

Energy density and power density have been widely used to evaluate the performance of SCs. Figure 4 compares the

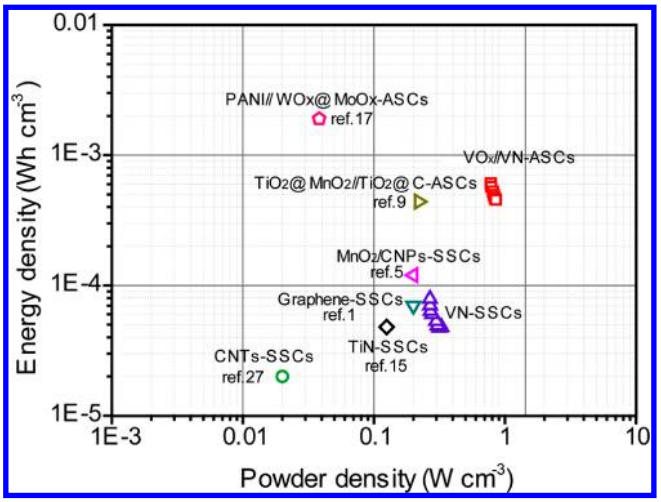

Figure 4. Ragone plots of the quasi-solid-state VO_x//VN-ASC devices measured in the gel electrolyte. The values reported for other SC devices are added for comparison.[1,5,9,15,17,27]

volumetric power and energy densities of the VN-SSCs and VO_x//VN-ASCs reported in this work to the values reported for other quasi/all-solid-state SCs (for detailed calculation, see the Supporting Information). The Ragone plot shows that the energy density and power density of the VO_x//VN-ASC device are considerably higher than those of VN-SSC devices measured at the same current density. For instance, the VO_x//VN-ASC device achieved a remarkable volumetric energy density of 0.61 mWh cm^{-3} at current density of 0.5 mA cm^{-2}, which is 7 times higher than that of the VN-SSC device (0.079 mWh cm^{-3}). Significantly, the volumetric energy density of the VO_x//VN-ASC is also substantially higher than those of recent reported quasi/all-solid-state SCs,[1,5,9,15,16,27] such as TiN-based SSCs (0.045 mWh cm^{-3}, PVA/KOH),[15] graphene-based SSCs (0.06 mWh cm^{-3}, PVA/H_3PO_4),[1] MnO_2/carbon particles (CNPs)-based SSCs (0.09 mWh cm^{-3}, 0.5 mA cm^{-2}, PVA/H_3PO_4),[5] and hydrogenated TiO_2@MnO_2//TiO_2@C-based ASCs (0.30 mWh cm^{-3}, 0.5 mA cm^{-2}, PVA/LiCl).[9] More importantly, the VO_x//VN-ASC device also exhibit a superior power density 0.85 W cm^{-3} at current density of 5 mA cm^{-2}, which is higher than those values reported for most of quasi/all-solid-state SSCs[5,15,27] and ASCs.[9,16,17] Moreover, the VO_x//VN-ASC device achieved a maximum specific energy density of 2.1 Wh kg^{-1}, which is also considerably higher than others solid-state SCs.[5,9,12,13,15] By minimizing the thickness of the electrolyte and the carbon cloth substrate, the performance based on total mass of ASC device can be further improved.

In summary, an effective strategy has been developed to stabilize VN nanowire anode without sacrificing its electrochemical performance by using LiCl/PVA gel electrolyte. By suppressing the oxidation reaction and structural pulverization, the VN nanowire electrode exhibited remarkable cycling stability in LiCl/PVA gel electrolyte with a capacitance retention of 95.3% after 10 000 cycles, which is much higher than that (14.1%) obtained in 5 M LiCl aqueous electrolyte. Significantly, we have successfully demonstrated a high performance ASC device based on the stabilized VN nanowire anode and VO_x nanowire cathode. The VO_x//VN-ASC device achieved a maximum energy density of 0.61 mWh cm^{-3} at current density of 0.5 mA cm^{-2} and a maximum power density of 0.85 W cm^{-3} at current density of 5 mA cm^{-2}. These values are substantially enhanced compared to most of the reported quasi/all-solid-state SC devices. This work constitutes the first demonstration of using VN nanowires as high-energy anode, which could potentially improve the performance of energy storage devices.

■ ASSOCIATED CONTENT

Ⓢ Supporting Information

Synthetic and analytical methods, capacitive equations, SEM images, XPS and XRD spectra, EIS spectra, CV, charge/discharge curves, and Ragone plot. This material is available free of charge via the Internet at http://pubs.acs.org.

■ AUTHOR INFORMATION

Corresponding Author

*E-mail: chedhx@mail.sysu.edu.cn (Y.T.); yli@chemistry.ucsc.edu (Y.L.).

Notes

The authors declare no competing financial interest.

■ ACKNOWLEDGMENTS

Y.L. acknowledges the support of this work by U.S. NSF (DMR-0847786), UCSC faculty startup funds, and National Center for Electron Microscopy at Lawrence Berkeley National Laboratory, which is supported by the U.S. Department of Energy (DE-AC02-05CH11231). Y. X. Tong acknowledges the financial support of this work by the Natural Science Foundations of China (90923008, 21273290 and J1103305) and the Research Fund for the Doctoral Program of Higher Education of China (No. 20120171110043). X. H. Lu thanks the Academic New Artist Ministry of Education Doctoral Post Graduate (China) for China Scholarship Council financial support and The Sun Yat-Sen Innovative Talents Cultivation Program for Doctoral Graduate Student.

■ REFERENCES

(1) El-Kady, M. F.; Strong, V.; Dubin, S.; Kaner, R. B. *Science* **2012**, *335* (6074), 1326−1330.
(2) Yu, G. H.; Hu, L. B.; Vosgueritchian, M.; Wang, H. L.; Xie, X.; McDonough, J. R.; Cui, X.; Cui, Y.; Bao, Z. N. *Nano Lett.* **2011**, *11* (7), 2905−2911.
(3) Niu, Z. Q.; Luan, P. S.; Shao, Q.; Dong, H. B.; Li, J. Z.; Chen, J.; Zhao, D.; Cai, L.; Zhou, W. Y.; Chen, X. D.; Xie, S. S. *Energ. Environ. Sci.* **2012**, *5* (9), 8726−8733.
(4) Niu, Z.; Dong, H.; Zhu, B.; Li, J.; Hng, H. H.; Zhou, W.; Chen, X.; Xie, S. *Adv. Mater.* **2013**, *25* (7), 1058−1064.
(5) Yuan, L. Y.; Lu, X. H.; Xiao, X.; Zhai, T.; Dai, J. J.; Zhang, F. C.; Hu, B.; Wang, X.; Gong, L.; Chen, J.; Hu, C. G.; Tong, Y. X.; Zhou, J.; Wang, Z. L. *ACS Nano* **2012**, *6* (1), 656−661.

(6) Yu, G. H.; Hu, L. B.; Liu, N. A.; Wang, H. L.; Vosgueritchian, M.; Yang, Y.; Cui, Y.; Bao, Z. A. *Nano Lett.* **2011**, *11* (10), 4438−4442.
(7) Choi, B. G.; Chang, S. J.; Kang, H. W.; Park, C. P.; Kim, H. J.; Hong, W. H.; Lee, S.; Huh, Y. S. *Nanoscale* **2012**, *4* (16), 4983−4988.
(8) Yu, H.; Bai, Y.; Zong, X.; Tang, F. Q.; Lu, G. Q. M.; Wang, L. Z. *Chem. Commun.* **2012**, *48* (59), 7386−7388.
(9) Lu, X.; Yu, M.; Wang, G.; Zhai, T.; Xie, S.; Ling, Y.; Tong, Y.; Li, Y. *Adv. Mater.* **2013**, *25* (2), 267−272.
(10) Fu, Y.; Cai, X.; Wu, H.; Lv, Z.; Hou, S.; Peng, M.; Yu, X.; Zou, D. *Adv. Mater.* **2012**, *24* (42), 5713−5718.
(11) Meng, F.; Ding, Y. *Adv. Mater.* **2011**, *23* (35), 4098−4102.
(12) Zheng, H. M.; Zhai, T.; Yu, M. H.; Xie, S. L.; Liang, C. L.; Zhao, W. X.; Zhang, Z. S.; Lu, X. H. *J. Mater. Chem. C* **2013**, *1*, 225−229.
(13) Lu, X. H.; Zhai, T.; Zhang, X. H.; Shen, Y. Q.; Yuan, L. Y.; Hu, B.; Gong, L.; Chen, J.; Gao, Y. H.; Zhou, J.; Tong, Y. X.; Wang, Z. L. *Adv. Mater.* **2012**, *24* (7), 938−944.
(14) Yuan, L.; Xiao, X.; Ding, T.; Zhong, J.; Zhang, X.; Shen, Y.; Hu, B.; Huang, Y.; Zhou, J.; Wang, Z. L. *Angew. Chem., Int. Ed.* **2012**, *51* (20), 4934−4938.
(15) Lu, X.; Wang, G.; Zhai, T.; Yu, M.; Xie, S.; Ling, Y.; Liang, C.; Tong, Y.; Li, Y. *Nano Lett.* **2012**, *12* (10), 5376−5381.
(16) Gao, H.; Xiao, F.; Ching, C. B.; Duan, H. *ACS Appl. Mater. Interfaces* **2012**, *4* (12), 7020−7026.
(17) Xiao, X.; Ding, T. P.; Yuan, L. Y.; Shen, Y. Q.; Zhong, Q.; Zhang, X. H.; Cao, Y. Z.; Hu, B.; Zhai, T.; Gong, L.; Chen, J.; Tong, Y. X.; Zhou, J.; Wang, Z. L. *Adv. Energy Mater.* **2012**, *2* (11), 1328−1332.
(18) Xiao, J. W.; Yang, S. H. *J. Mater. Chem.* **2012**, *22* (24), 12253−12262.
(19) Yan, J.; Fan, Z. J.; Sun, W.; Ning, G. Q.; Wei, T.; Zhang, Q.; Zhang, R. F.; Zhi, L. J.; Wei, F. *Adv. Funct. Mater.* **2012**, *22* (12), 2632−2641.
(20) Qu, Q. T.; Yang, S. B.; Feng, X. L. *Adv. Mater.* **2011**, *23* (46), 5574−5580.
(21) Choi, D.; Blomgren, G. E.; Kumta, P. N. *Adv. Mater.* **2006**, *18* (9), 1178−1182.
(22) Choi, D. W.; Kumta, P. N. *Electrochem. Solid-State Lett.* **2005**, *8* (8), A418−A422.
(23) Glushenkov, A. M.; Hulicova-Jurcakova, D.; Llewellyn, D.; Lu, G. Q.; Chen, Y. *Chem. Mater.* **2010**, *22* (3), 914−921.
(24) Zhang, L.; Holt, C. M. B.; Luber, E. J.; Olsen, B. C.; Wang, H. T.; Danaie, M.; Cui, X. W.; Tan, X. H.; Lui, V. W.; Kalisvaart, W. P.; Mitlin, D. *J. Phys. Chem. C* **2011**, *115* (49), 24381−24393.
(25) Ghimbeu, C. M.; Raymundo-Pinero, E.; Fioux, P.; Beguin, F.; Vix-Guterl, C. *J. Mater. Chem.* **2011**, *21* (35), 13268−13275.
(26) Wang, G.; Lu, X.; Ling, Y.; Zhai, T.; Wang, H.; Tong, Y.; Li, Y. *ACS Nano* **2012**, *6* (11), 10296−10302.
(27) Kaempgen, M.; Chan, C. K.; Ma, J.; Cui, Y.; Gruner, G. *Nano Lett.* **2009**, *9* (5), 1872−1876.
(28) Xie, K.; Qin, X. T.; Wang, X. Z.; Wang, Y. N.; Tao, H. S.; Wu, Q.; Yang, L. J.; Hu, Z. *Adv. Mater.* **2012**, *24* (3), 347−352.
(29) Yuan, D. S.; Zhou, T. X.; Zhou, S. L.; Zou, W. J.; Mo, S. S.; Xia, N. N. *Electrochem. Commun.* **2011**, *13* (3), 242−246.
(30) Zhou, X. P.; Chen, H. Y.; Shu, D.; He, C.; Nan, J. M. *J. Phys. Chem. Solids* **2009**, *70* (2), 495−500.
(31) Levinson, D. W. *Acta Metall.* **1955**, *3* (3), 294−295.
(32) Loehman, R. E.; Rao, C. N. R.; Honig, J. M. *J. Phys. Chem.* **1969**, *73* (6), 1781−1784.
(33) Swiatowska-Mrowiecka, J.; Maurice, V.; Zanna, S.; Klein, L.; Marcus, P. *Electrochim. Acta* **2007**, *52* (18), 5644−5653.
(34) Engstrom, A. M.; Doyle, F. M. *J. Power Sources* **2013**, *228*, 120−131.